SCIENTIFIC REPORTS

OPEN

Cooling field and temperature dependent exchange bias in spin glass/ferromagnet bilayers

Received: 21 May 2015
Accepted: 03 August 2015
Published: 08 September 2015

W. B. Rui[1], Y. Hu[2,5], A. Du[2], B. You[1,4], M. W. Xiao[1], W. Zhang[1], S. M. Zhou[3] & J. Du[1,4]

We report on the experimental and theoretical studies of cooling field (H_{FC}) and temperature (T) dependent exchange bias (EB) in $Fe_xAu_{1-x}/Fe_{19}Ni_{81}$ spin glass (SG)/ferromagnet (FM) bilayers. When x varies from 8% to 14% in the Fe_xAu_{1-x} SG alloys, with increasing T, a sign-changeable exchange bias field (H_E) together with a unimodal distribution of coercivity (H_C) are observed. Significantly, increasing in the magnitude of H_{FC} reduces (increases) the value of H_E in the negative (positive) region, resulting in the entire $H_E \sim T$ curve to move leftwards and upwards. In the meanwhile, H_{FC} variation has weak effects on H_C. By Monte Carlo simulation using a SG/FM vector model, we are able to reproduce such H_E dependences on T and H_{FC} for the SG/FM system. Thus this work reveals that the SG/FM bilayer system containing intimately coupled interface, instead of a single SG layer, is responsible for the novel EB properties.

Recently, spin glasses (SG) have attracted much attention and stimulated intensive studies because the combination of quenched spin spatial randomness and frustration create a complex free energy landscape with multiple local energy minima and finding the stable spin states formidable challenging[1–3]. In spite of many theoretical attempts of developing renormalization group[1,4], mean-field approximation[5] and Monte Carlo simulation[3,6–8] based analyses, the low-temperature (T) spin phases as well as the out-of-equilibrium aging dynamics of such materials remain matters of strong debates. Not surprisingly, the complex nature of SG spin structures gives rise to the unique and diverse macroscopic properties in many fields of science. Exchange bias (EB) for ultrahigh-density magnetic recording is one of such areas[9].

The EB effect in coupled ferromagnet (FM)/antiferromagnet (AFM) system has been studied extensively because of its critical role in spintronic devices and intriguing spin physics. The EB phenomenon manifests itself as a shifted and broadened magnetization-applied field (M-H) hysteresis loop along the H axis when FM/AFM systems are cooled below an EB blocking temperature (T_B) under an external magnetic cooling field (H_{FC})[10,11]. Therefore, EB is both H_{FC}- and T-dependent normally. Most of the EB studies show that large enough H_{FC} can either saturate a negative EB field (H_E) for FM typed interfacial couplings ($J_{IF} > 0$)[12,13] or induce a positive H_E for AFM typed J_{IF} (< 0)[14–16]. On the other hand, the thermal energy at high T will weaken J_{IF}, and thus H_E often decreases monotonically with increasing T and finally vanishes at T_B. Under certain circumstances, a sign inversion of H_E, i.e., a small positive EB, can be observed in a narrow T region just below T_B for some EB systems[17,18]. These abnormal phenomena are argued to be a result of the unidirectional coercivity (H_C) enhancement along the H_{FC} direction. Observation of this effect requires a modest H_{FC} and it has been only reported in quite few AFM based materials since the origin of positive EB is very different from systems with negative J_{IF}[14]. Therefore, the study of H_{FC} together with T dependences of EB is of critical importance for the understanding of EB mechanism.

[1]National Laboratory of Solid State Microstructures and Department of Physics, Nanjing University, Nanjing 210093, P. R. China. [2]College of Sciences, Northeastern University, Shenyang, 110819, P. R. China. [3]Department of Physics, Tongji University, Shanghai, 200092, P. R. China. [4]Collaborative Innovation Center of Advanced Microstructures, Nanjing, 210093, P. R. China. [5]MOE Key Laboratory for Anisotropy and Texture of Materials, Northeastern University, Shenyang, 110819, P. R. China. Correspondence and requests for materials should be addressed to Y.H. (email: huyong@mail.neu.edu.cn) or J.D. (email: jdu@nju.edu.cn)

As mentioned previously, when SG is involved, the EB dependences on H_{FC} and T can be different from conventional FM/AFM systems. Nayak *et al.*[19] found that zero-field-cooled (ZFC, $H_{FC}=0$) H_E in Heusler compound Mn_2PtGa is comparable to the field-cooled (FC) value, due to the coexistence of field-induced irreversible magnetic behavior and a SG-like phase. Sabyasachi *et al.*[20] found that even a strong H_{FC} of 80 kOe cannot saturate the H_C of nanocrystalline $La_{1/3}Sr_{2/3}FeO_{3-\delta}$ at 5 K and this behavior was ascribed to the randomness of glassy magnetic phase. Especially, by using a canonical SG alloy (CuMn), Ali *et al.*[21] first reported the sign-changeable behavior of T-dependent H_E in SG/FM bilayer systems. Subsequently, Yuan *et al.*[22] and Ali *et al.*[23] observed the similar $H_E \sim T$ trend in other SG materials (FeAu and FeCr). Without performing any H_{FC}-dependent studies, they interpreted those abnormal T-dependent EB behaviors either in the framework of the Ruderman-Kittel-Kasuya-Yosida (RKKY) interaction theory[21,22] or by considering the existence of a T-driven SG-to-AFM phase transition[23]. However, due to the diverse and entangled spin interactions existed in SG and the fact these interactions can be affected by the field cooling process, the T-dependent sign-changeable H_E should be greatly influenced by H_{FC} in the SG/FM bilayers. Theoretically, Usadel and Nowak[24] have attempted to reproduce the EB phenomena in the SG/FM bilayer systems by applying an Ising model considering a short-range Gaussian distribution of interactions to simulate the SG material. While they were able to predict the decrease in the magnitude of H_E at low T when increasing H_{FC}, the model failed to obtain the $H_E \sim T$ behaviors as seen in Ref. 21–23. To the best of our knowledge, the *experimental* observations of the H_{FC} dependence of EB in SG/FM bilayer systems has remained unreported yet, and there are no *unified* non-phenomenological models that can interpret both the T and H_{FC} dependences of EB in SG based systems.

In this paper, the effects of H_{FC} and T on EB in the FeAu/NiFe SG/FM bilayers were first investigated experimentally. Phenomena of H_E sign inversion at the temperatures just below T_B, the decrease (increase) in H_E magnitude with increasing H_{FC} at low T (high T), the unimodal distribution of H_C against T, and the H_{FC}-independent H_C have all been observed. Then using Monte Carlo technique, we exploited a short-range SG vector model, with a combination of disorder and frustration as well as thermodynamic relaxation and successfully reproduced and interpreted the EB phenomena governed by H_{FC} and T. Distinct from the AFM based systems, this study suggests that the EB effect and especially the sign-changeable (positive EB) behavior in the narrow T region just below T_B in the SG/FM bilayer systems may be inherent, and exists in all exchange biased SG/FM bilayers.

Results

The quantities of H_E and H_C are calculated based on $H_E=(H_{C1}+H_{C2})/2$ and $H_C=(-H_{C1}+H_{C2})/2$, where H_{C1} and H_{C2} denote the coercive fields at the descending and the ascending branches of the M-H hysteresis loop, respectively. The temperature dependences of H_E and H_C in Fe_xAu_{1-x}/FeNi bilayers are shown in Fig. 1, where $x=4\%$, 8%, 11% and 14% and H_{FC} is 5 kOe for these measurements. In order to confirm the SG nature of the FeAu layers, ZFC-FC curves were measured with an applied field of 50 Oe. The inset in Fig. 1 shows typical features of spin glass behaviors for a FeAu single layer with $x=11\%$. The value of the freezing temperature (T_F) for this sample is about 30 K, below which the ZFC and FC curves become bifurcated. DC memory effect[25] has also been observed in this sample (not shown), providing a further proof of the SG state. Similar SG behaviors can be found in all other FuAu single layer films with x varying from 4% to 14%.

Figure 1(a) shows a clear sign-change in H_E versus T in the Fe_xAu_{1-x}/FeNi bilayers with $x=8\%$, 11% and 14%. With increasing T from the lowest value of 2 K, H_E increases abruptly from a negative value and changes its sign at T_0, which is named the compensation temperature[21–23]. When T is increased further, H_E increases to a positive maximum at another temperature defined as T_P. After that, H_E decreases gradually and falls below to zero when T approaches to T_B. As for the H_C dependence on T, it increases initially with T and also shows a concurrent peak at around T_P, as shown in Fig. 1(b). It is noteworthy that H_E shows a maximum positive value of about 40 Oe when $x=8\%$, much larger in magnitude than any other previous reported results (normally less than 10 Oe), even for a thin FM layer of 2.2 nm in ref. 21. However, the sign-changeable behavior of H_E with T is absent when $x=4\%$, possibly because the value of T_0 is lower than 2 K and beyond the present temperature measuring range.

Figure 1 unambiguously demonstrates that for the SG/FM bilayers the $H_E \sim T$ curve depends strongly on the composition of the SG layer. Previously, such sign-changeable behavior of H_E against T was explained by the competition between long-range oscillatory RKKY couplings from the spins deep inside the SG layer and those close to the interface[21,22]. In the present work, besides reconsidering the sign-changeable behavior, we focus on studying the H_E and H_C influenced by H_{FC}. First we discuss the evolution of M-H hysteresis loops versus T. Figure 2 shows the M-H hysteresis loops obtained between 2 K and 20 K for the Ta(4 nm)/$Fe_{11}Au_{89}$(50 nm)/FeNi(5 nm)/Ta(2 nm) sample, after cooled from 300 K to 2 K under $H_{FC}=50$ kOe. The M-H hysteresis loop measured at 2 K clearly shows that a negative EB was established after field cooling. As shown in Fig. 2(a), when T increases from 2 K to 7 K, the ascending branch of the hysteresis loop shifts rightwards while the descending branch keeps almost unchanged. With further increasing in T from 8 K to 20 K, as displayed in Fig. 2(b), the hysteresis loop shrinks from both sides towards the center but the shift of ascending branch is more significantly than the descending branch. Therefore, the different T-dependent variation behaviors of the two loop branches lead to the concurrent peak on both the $H_E \sim T$ and $H_C \sim T$ curves, coinciding with the appearance of $T_P \sim 7$ K as

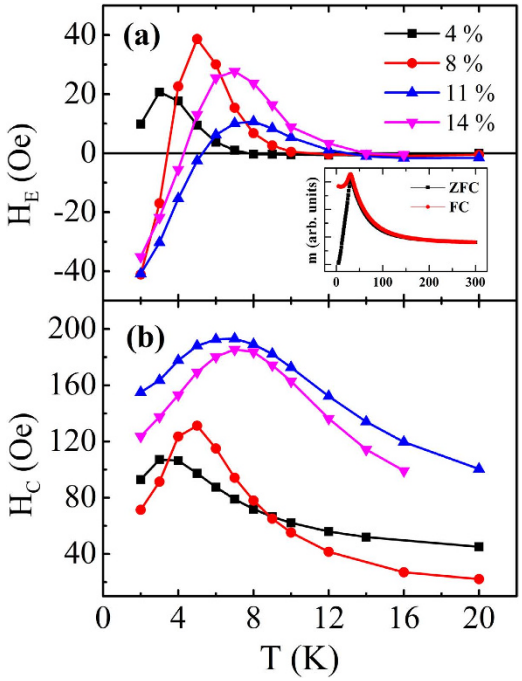

Figure 1. Temperature dependent H_E (a) and H_C (b) with a cooling field of $H_{FC} = 5$ kOe for Fe_xAu_{1-x}(50 nm)/FeNi(5 nm) bilayers with $x = 4\%$, 8%, 11% and 14%. The inset shows the ZFC-FC magnetization curves for the $Fe_{11}Au_{89}$(50 nm) film under $H_{FC} = 50$ Oe with T varying between 5 K to 300 K.

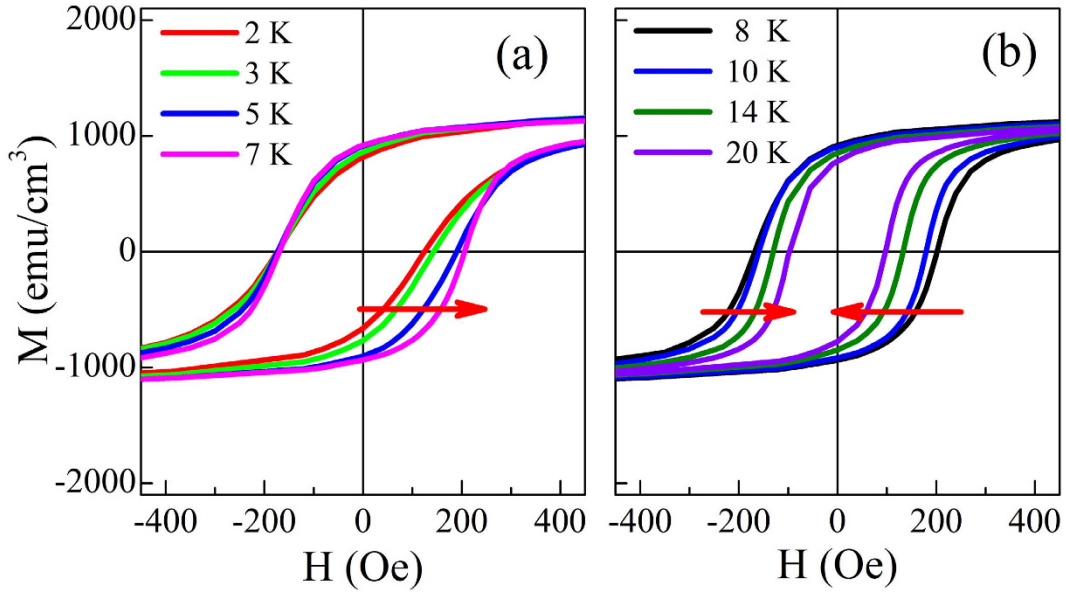

Figure 2. The *M-H* hysteresis loops measured for a $Fe_{11}Au_{89}$(50 nm)/FeNi(5 nm) sample in the temperature range of 2 K–7 K (a) and 8 K–20 K (b). The arrows are guides to eyes, indicating the direction of loop shift.

shown in Fig. 1. These results indicate that the T-dependent magnetization reversal mechanisms and/or the thermodynamic spin relaxation at the descending and ascending branches may be quite different.

Experimental study of the H_{FC} dependent EB has been performed and representative results are presented in Fig. 3. As displayed in Fig. 3(a,c), when H_{FC} increases from 0.2 kOe to 50 kOe, the $H_E \sim T$ curve shifts toward upper-left while the $H_C \sim T$ curves keep almost overlapped. Accordingly, T_0 decreases from 5.5 K to 4.2 K. The peak position of the $H_E \sim T$ curve moves towards lower T slightly and the maximum positive value of H_E increases significantly from 10 Oe to 18 Oe. Figure 3(b,d) show the corresponding

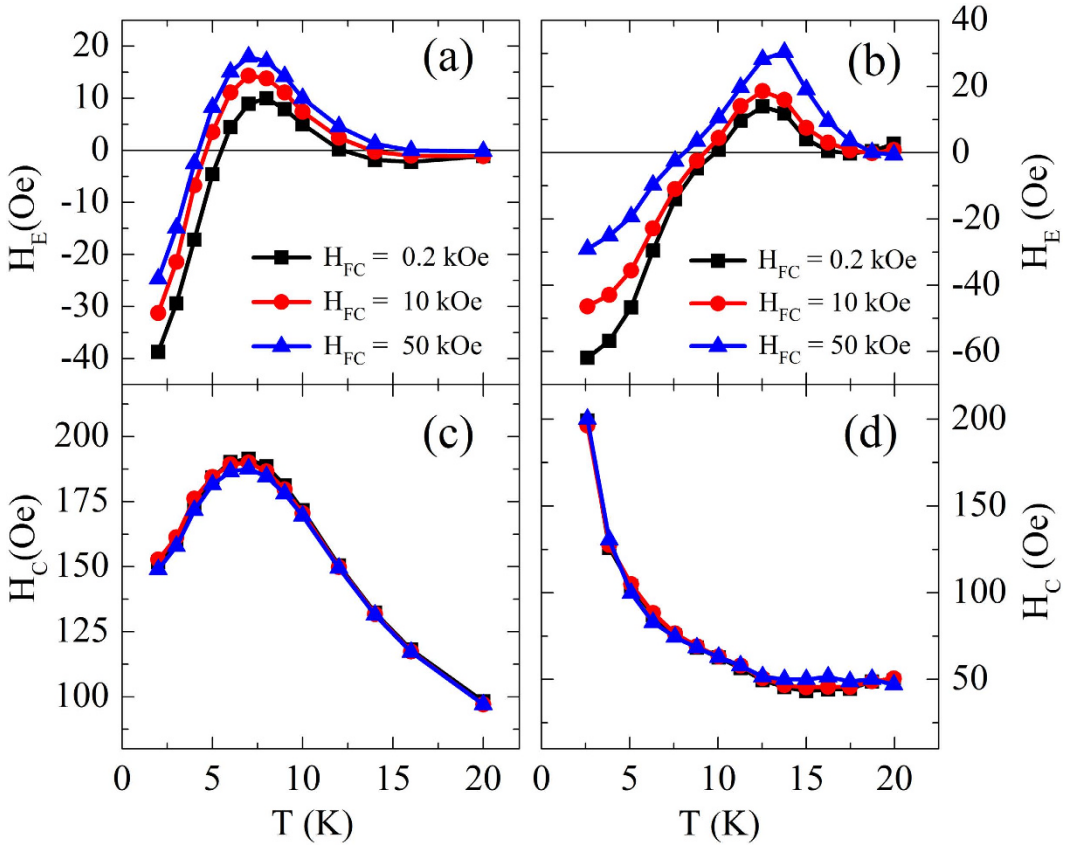

Figure 3. Cooling field influence on the temperature dependent H_E (a) and H_C (c) for a $Fe_{11}Au_{89}$(50 nm)/FeNi(5 nm) sample measured between $T = 2$ K and 20 K and the corresponding calculated results of H_E (b) and H_C (d) for the SG/FM bilayers obtained between $T = 2.6$ K and 19.96 K.

simulation results. The sign inversion in H_E with T can be reproduced and $H_E \sim T$ curve shift can also be repeated. It is noticed that simulated T_0, T_P, and $H_E(T_P)$ results have certain deviation from the experiments, but the theoretical $H_E \sim T$ curves agree well with experimental measurements. On the other hand, the calculated trend of H_C versus T is different from the experimental results obtained both by Ali *et al.*[21] and us, but in agreement with those reported in ref. 22. Another disagreement with the present experimental results is that the theoretical $H_C \sim T$ curves are H_{FC}-dependent at the temperatures just below T_B, i.e., H_C for larger H_{FC} is slightly larger. These discrepancies will be addressed later.

At low T, the H_{FC} dependence of H_E is also interesting. The experimental and simulation results as shown in Fig. 4 indicate that the entire M-H hysteresis loop moves rightwards with a strong enough H_{FC}. As a result, H_E decreases with increasing H_{FC} while H_C is insensitive to H_{FC}. Furthermore, there is a slight vertical magnetization shift observed experimentally under strong H_{FC}, arising from a minor magnetization in the FeAu SG. Increase in H_E at low H_{FC} (≤ 1 kOe) is very small because saturation in the FeNi (FM) has not been achived.

Based on the consistent H_E results between experiment and simulation, we interpret the above experimental phenomena relying on our simulation method. At first, we have excluded that the EB phenomena in the SG/FM bilayers depend solely on interfaces [see Supplementary Material A]. In other words, the configurations/spins inside the SG influence the FM spins through the SG/FM interface and the SG/FM interface itself also plays a significant role in establishing EB. Thus in the low T region, we calculate the interfacial exchange energy density (ε_{IF}) to interpret the relative EB behavior, which can be expressed as

$$\varepsilon_{IF} = -\frac{1}{A} J_{IF}^{ij} \sum_{<i \in FM, j \in SG>} \boldsymbol{\mu}_i \cdot \boldsymbol{\mu}_j, \quad (1)$$

where J_{IF}^{ij} is the interfacial coupling stength between the FM and SG spins, A is the interface area and $\boldsymbol{\mu}$ denotes the magnetic moment of the interfacial spin belonging to the FM or SG. Since this is the dominant energy term influencing the H_E in SG/FM bilayers and meanwhile a low enough T will suppress thermal fluctuation, the change of ε_{IF} mainly determines the evolution of spin configuration at the interface during isothermally magnetizing at low T. Therefore, it provides us the opportunity to image the

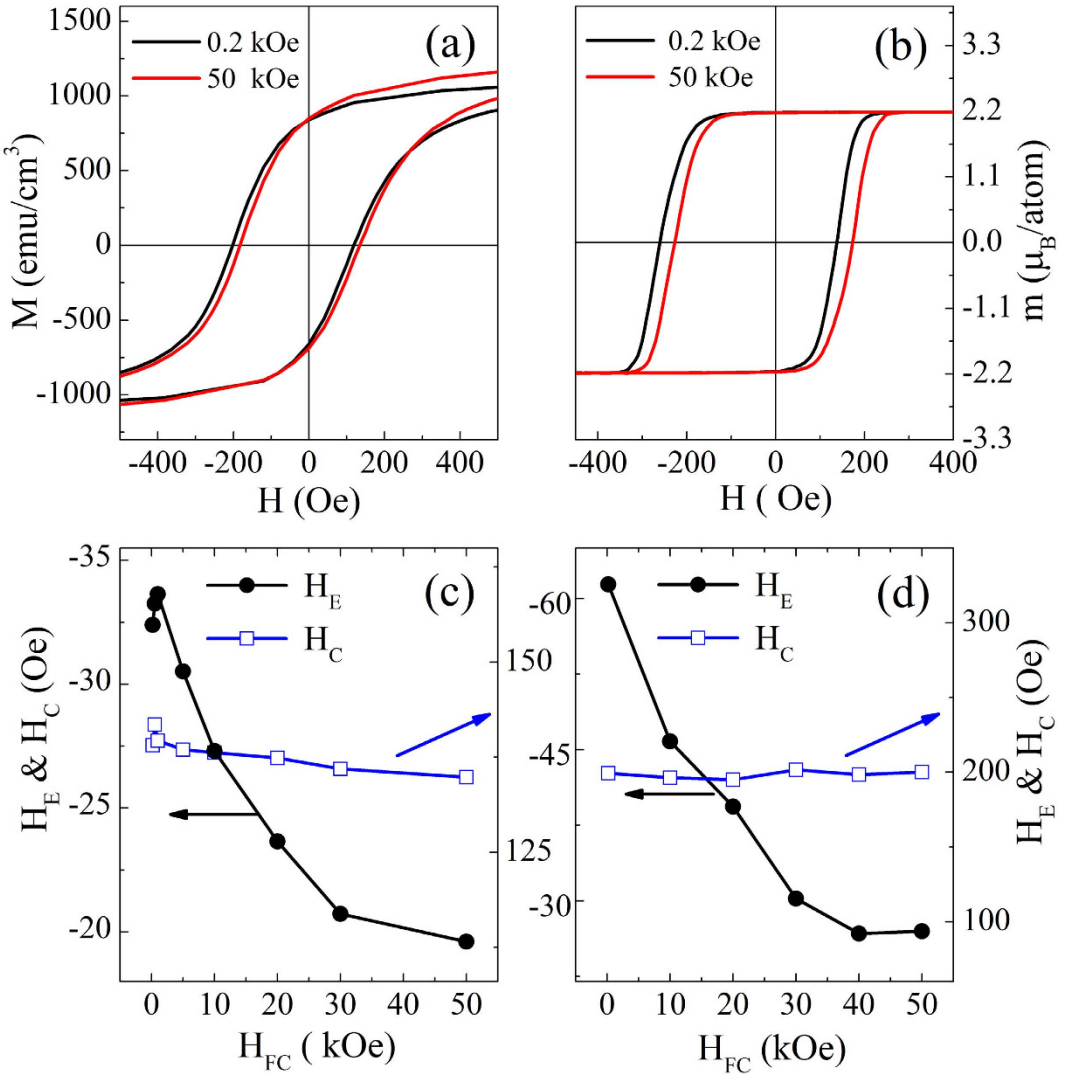

Figure 4. (**a**) The *M-H* hysteresis loops measured under $H_{FC} = 0.2$ kOe and 50 kOe at $T = 2$ K for a $Fe_{11}Au_{89}$(50 nm)/FeNi(5 nm) sample, (**b**) the calculated *M-H* hysteresis loops under $H_{FC} = 0.2$ kOe and 50 kOe at $T = 2.6$ K for the SG/FM bilayers, and the experimental (**c**) and calculated (**d**) cooling field dependences of low-temperature H_E and H_C.

M-H behaviors microscopically and helps us to elucidate how H_E is influenced by H_{FC}. Figure 5(a) shows the results calculated for $T = 2.6$ K. In addition, other parameters including the spin energy barrier and the *x* component of spin under specific fields are calculated simultaneously in order to provide a clear physical picture during isothermally magnetizing at low *T*, with the results shown in Fig. 5 (b,c), respectively.

At low *T* after field cooling, as shown in Fig. 5(a), ε_{IF} for $H_{FC} = 50$ kOe is higher than that for $H_{FC} = 0.2$ kOe, and the value of ε_{IF} keeps constant with decreasing *H* in the positive direction. Then *H* changes its sign and increases in magnitude, and the value of ε_{IF} begins to decrease around $H = -100$ Oe. For $H_{FC} = 0.2$ kOe, ε_{IF} can reduce to a lower value. With further increase in *H* along the negative direction, ε_{IF} begins to increase, corresponding to the magnetization reversal at the descending branch, and then reaches a comparable stable value both for $H_{FC} = 0.2$ kOe and 50 kOe. After the reversal, ε_{IF} is unchanged approximately again so long as *H* is applied in the negative direction. Once *H* turns back to the positive direction and increases exceeding 100 Oe, ε_{IF} decreases rapidly for both H_{FC} accompanied by magnetization reversal at the ascending branch. Moreover, the rapid decrease of ε_{IF} occurs at a larger *H* for $H_{FC} = 50$ kOe.

The above hysteretic behavior of calculated ε_{IF} and the H_{FC} dependent EB at low T ($T < T_0$) can be understood as follows. After field cooling, the bilayers undergone different H_{FC} possess different ε_{IF}, as a result of the competition between H_{FC} and J_{IF}. Meantime, the competition also establishes a H_{FC} dependent energy barrier (E_b) configuration, as shown in Fig. 5(b). These energy barriers confine spin rotation, and E_b for $H_{FC} = 50$ kOe is apparently higher than that for $H_{FC} = 0.2$ kOe. The reason is that H_{FC} is applied

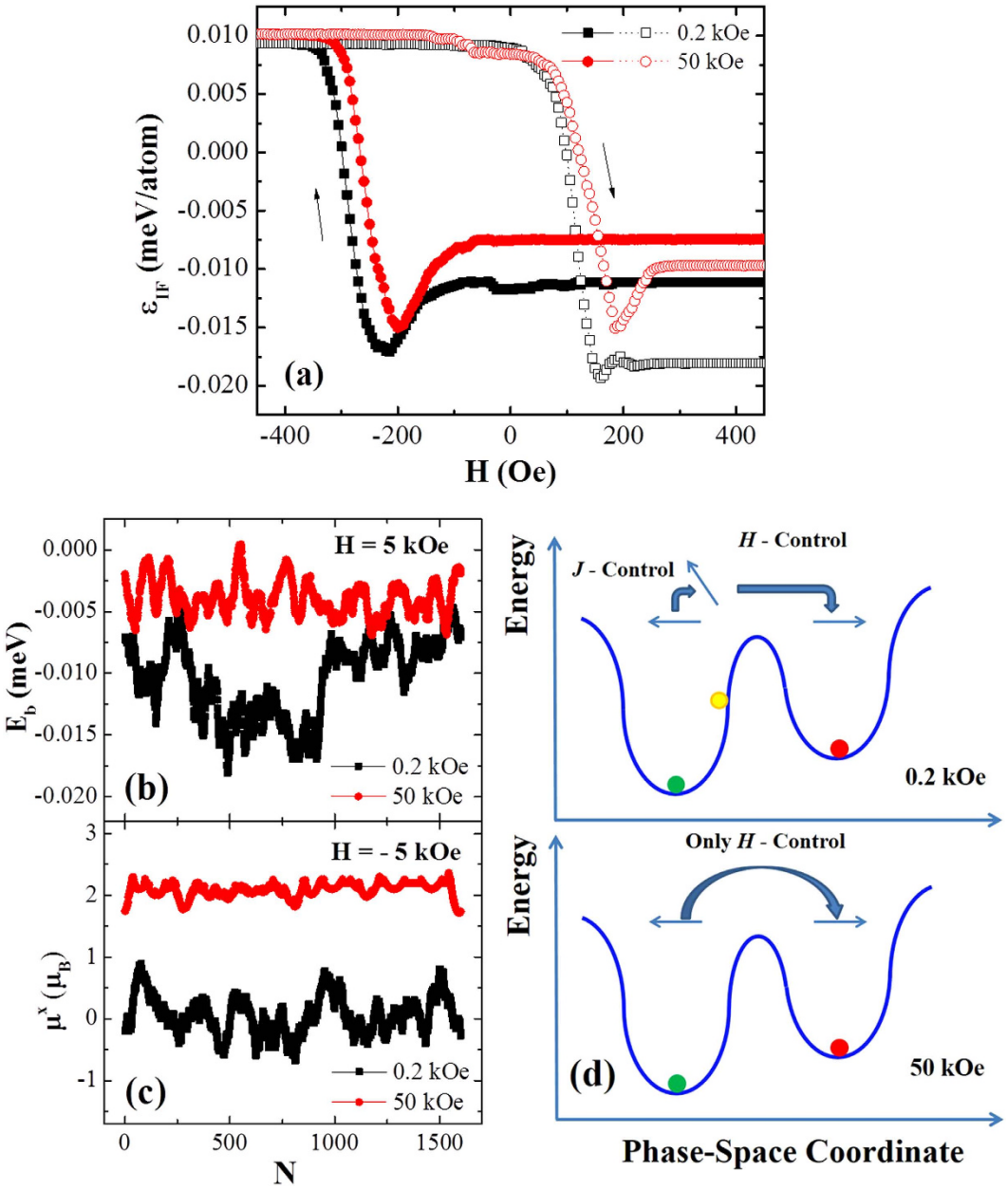

Figure 5. (**a**) Calculated interfacial exchange energy density (ε_{IF}) during the magnetizing process at $T = 2.6$ K after cooling under $H_{FC} = 0.2$ kOe and 50 kOe, where solid symbols-solid lines and open symbols-dot lines correspond to the descending and ascending branches of the *M-H* hysteresis loops and arrows indicate the magnetizing directions. (**b**) Calculated energy barriers (E_b) of the SG spins at the interface at $T = 2.6$ K after the field cooling process and before the isothermally magnetizing. (**c**) Calculated *x* component (μ^x) of the SG magnetic moments at the interface under $H = -5$ kOe during the magnetizing process at $T = 2.6$ K. (**d**) Schematic illustrations of the energy versus phase-space coordinate during the magnetization reversal at the ascending branch of the *M-H* hysteresis loops.

along with the SG anisotropy and high H_{FC} drags more spins to align with it, so the anisotropy energy of these spins is minimized simultaneously. This will result in a higher E_b according to the Stoner-Wohlfarth theory. When H decreases along the direction of H_{FC}, no extra energy is required to change the configurations of bilayers, and the systems are called in frozen states. When H reverses its direction to become opposite to H_{FC} (termed negative direction), there is a critical field ($H \approx -100$ Oe) beyond which the spins in the FM single layer can be reversed[24]. However, in the SG/FM bilayers the SG spins, via J_{IF}, can impede this process, while the interfacial spins still tend to rearrange towards low exchange energy direction. The rearrangement of SG spin is also influenced by E_b and thus ε_{IF} for $H_{FC} = 0.2$ kOe decreases to a lower value. It is worth noting that the lower the ε_{IF} is, the tighter is the bond between spins. To reverse

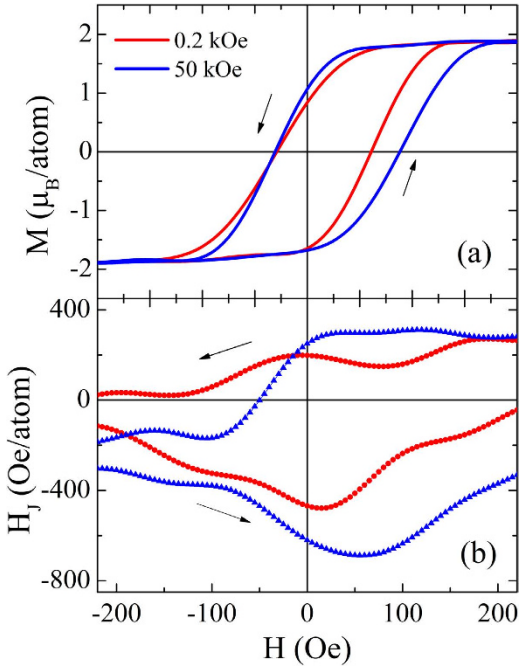

Figure 6. (**a**) Calculated *M-H* hysteresis loops at $T = 12.52$ K after cooling under $H_{FC} = 0.2$ kOe and 50 kOe, and (**b**) the corresponding calculated interfacial exchange fields (H_J) as a function of magnetic field, where arrows indicate the magnetizing directions.

the FM spins to the negative direction, larger H is needed for $H_{FC} = 0.2$ kOe to overcome the exchange energy. Hence the magnitude of H_{C1} for $H_{FC} = 0.2$ kOe is larger than that for $H_{FC} = 50$ kOe.

When the magnetization reversal at the descending branch is accomplished, ε_{IF} is increased abruptly up to a nearly identical value for both H_{FC} and the bilayer spin configuration become frozen again. We have to resort to other approaches to interpret the subsequent magnetizing process. Accordingly, the SG spin orientations at the interface (denoted by μ^x) under large negative H are calculated and shown in Fig. 5(c), and $\mu^x = 2.2\,\mu B$ indicates that the spins are aligning with H_{FC} while $\mu^x = 0$ means that the spins are perpendicular to H_{FC}. Remarkably, the SG spins for $H_{FC} = 0.2$ kOe show random orientations in the film plane, whereas for $H_{FC} = 50$ kOe all spins keep aligning with H_{FC}, although in both cases ε_{IF} has almost the same value. The spin configuration difference under different H_{FC} will influence the magnetization reversal at the ascending branch around $H = 100$ Oe. For $H_{FC} = 0.2$ kOe, randomly oriented SG spins are more easily to drag the FM spins to deviate from the negative field direction via J_{IF} under weak H, minimizing the interfacial exchange energy. It resembles that J_{IF} favors the reduction in the reversal field of FM spin, as illustrated in the top panel of Fig. 5(d). In comparison, for $H_{FC} = 50$ kOe, collinearly aligned SG spins couple to the FM spins via positive or negative J_{IF}. For the FM spins pointing to the negative field direction, the interfacial coupling with negative J_{IF} restrains the FM reversal while positive J_{IF} favors the FM reversal. However, the FM reversal for positive J_{IF} must overcome the ansotropy energy. Therefore, in both cases J_{IF} demotes FM reversal, and thus the FM reversal is driven only by H [see the bottom panel of Fig. 5(d)]. As a result, H_{C2} for $H_{FC} = 0.2$ kOe is smaller than that for $H_{FC} = 50$ kOe and H_E for $H_{FC} = 0.2$ kOe is more pronounced.

On the other hand, the influence of H_{FC} on H_C at low T will be briefly discussed here. It is well-known that H_C is determined by the density of pinned sites, such as defects, which controls the nucleation and propagation of domain walls in FM[26,27]. In the present SG/FM bilayers, H_C also depends on the SG spin behaviors at the interface[28]. As mentioned above, H_{FC} can reduce $|H_{C1}|$ while enhance H_{C2}. We speculate that the decrement of $|H_{C1}|$ and the increment of H_{C2} are comparable due to invariable E_b during isothermally magnetizing. Therefore, H_C becomes H_{FC}-independent.

When the *M-H* hysteresis loops are measured at the temperatures between T_0 and T_B ($T_0 < T < T_B$), H_E may change its sign to become positive and its magnitude is also H_{FC}-dependent. However, in contrast to $T < T_0$, now H_E increases with increasing H_{FC}, as the results calculated at $T = 12.52$ K shown in Fig. 6(a). The *M-H* hysteresis loop for $H_{FC} = 50$ kOe has a larger width and shifts more towards right than that for $H_{FC} = 0.2$ kOe. For the phenomenon of positive H_E in this T region, some mechanisms have been proposed. For example, it was attributed to the AFM interfacial coupling[14–16] or unidirectional coercive field enhancement along the H_{FC} direction in AFM/FM bilayers. It was also argued that the positive H_E in SG/FM bilayers is directly due to the RKKY type interaction influenced by T to a different extent[21,22] or the T-driven SG-to-AFM phase transition[23]. However, all these interpretations lack microscopic evidence and do not take into account the influence of H_{FC} on positive H_E.

Different from the case of low T, thermal fluctuations are enhanced at these temperatures, although the SG spins can be still frozen below T_F. Especially for the FM spins with weak anisotropy, their orientations will be randomized by thermal energy, so ε_{IF} cannot well describe the behaviors of SG spins and is no longer suitable to interpret the phenomena at these temperatures. Therefore, we turn to calculate the average interfacial exchange field (H_J), which arises from the SG and interacts with the FM spins through the interface as

$$H_J = \frac{1}{A}\sum_{i\in FM} J_{IF}^{ij}\boldsymbol{\mu}_j. \quad (2)$$

Here J_{IF}^{ij} is the interfacial coupling between the FM and SG spins, A is the interface area and $\boldsymbol{\mu}_j$ represents the magnetic moment of the SG spins at the interface that are directly coupled to the FM spin. Apparently, H_J is influenced by the SG and thus is T- and H-dependent. As shown in Fig. 6(a,b), H_J remains positive until H_{C1} and then changes to negative before H_{C2}. Similar to the external magnetic field effect, H_J favors the spins to align with it and thus impedes the H-driven magnetization reversals for both branches. For $H_{FC} = 0.2$ kOe or 50 kOe, $|H_J|$ in the fourth quadrant is generally larger than that in the second quadrant with same applied magnetic field, i.e. $|H_J\ (-H_{C1})| > |H_J\ (H_{C1})|$. Hence a larger H is needed to realize magnetization reversal at the ascending branch, i.e., H_{C2} is larger than $|H_{C1}|$. It results in positive H_E. For larger H_{FC} of 50 kOe, H_J before H_{C1} is close to that for $H_{FC} = 0.2$ kOe, leading to similar H_{C1} for both H_{FC}. However, in the fourth quadrant, $|H_J|$ for $H_{FC} = 50$ kOe is much larger than that for $H_{FC} = 0.2$ kOe [see Fig. 6(b)], leading to a larger H_{C2} [see Fig. 6(a)]. Consequently, the positive H_E is larger for higher H_{FC}.

Discussion

Different from conventional AFM/FM bilayers, the spin configuration can be rearranged in the present FeAu/FeNi (SG/FM) bilayers even at very low T (e.g. 2 K) due to intrinsic randomness and frustration in the SG layer. Significantly, our work reveals that this reconfiguration can be controlled by H_{FC} and behaves quite differently in different T regions. When $T < T_0$, the spin reconfiguration in the SG can easily occur. For small H_{FC}, the polarization of SG is weak. In the SG/FM bilayers, a saturated FM layer will couple to the SG spins unidirectionally and result in prominent asymmetry of FM reversal at both branches of an M-H loop and a negative H_E. However, for large H_{FC}, the polarization of SG is enhanced, impeding the reconfiguration process. Thus the asymmetry of FM reversal is weakened and H_E decreases. The experimental and theoretical findings are both consistent with the explanations proposed by Usadel and Nowak[24]. On the other hand, when $T_0 < T < T_B$, the thermal fluctuation cannot be ignored and even may smear out other energy landscapes. The ε_{IF} adopted at the low T below T_0 is not suitable for the explanation of positive EB effect. Therefore, more direct effect from SG to FM, i.e. H_J is considered. Positive (negative) H_J favors the FM spins to align with (against) H_{FC} and thus forms FM (AFM) type interfacial coupling to the FM spins along the H_{FC} direction. As the calculated results of H_J shown in Fig. 6(b), an FM-to-AFM transition type of interfacial couplings does occur and this process is H-driven, which is different from the T-driven phase transition model suggested by Ali *et al.*[23]. Hence a positive H_E appears when $T_0 < T < T_B$. Moreover, although the thermal fluctuation deteriorates thermal stability, large H_{FC} leads to strong polarization of SG and enhance the system stability, which is beneficial to H_J and favors enhancement in H_E [see Fig. 6]. As a result, the positive EB for large H_{FC} is more obvious than that for small H_{FC}.

Now we will discuss some of discrepancies between experiment and simulation briefly. In the actual FeAu/FeNi bilayers, when T is decreased, the exchange and anisotropy energies are enhanced gradually to induce H_E below T_B and this process also contributes to H_C enhancement. With further decreasing T, due to the polycrystalline nature of the FM layer, the easy axes of the FM grains cannot fully lie along with the magnetizing direction, leading to reduction of H_C. Therefore, the variation of H_C versus T is non-monotonic. In the present simulation, a single crystal model including a uniaxial anisotropy and a saturated FM was adopted to study the EB properties and the magnetizing directions were set to be along with the easy axis. Therefore, the calculated M-H hysteresis loops are more rectangle-shaped and the calculated values of H_E or H_C are larger than those obtained from experiments. Significantly, the increase of anisotropy energy at low T in the simulation further contributes to the increase of H_C when the M-H hysteresis loops are measured along the easy-axis direction. As a result, H_C has a monotonic and sharp increase with decreasing T. Also, due to the saturated FM in the initial state, the experimental result of increase in H_E with initially increasing H_{FC} is not obtained in simulation. Since the model only considers the most dominant energy terms concerning EB, a perfect agreement between theory and experiment cannot be achieved.

To summarize, the dependence of EB properties in FeAu/FeNi SG/FM bilayers on H_{FC} and T have been studied experimentally and numerically. A sign-changeable behavior of H_E versus T is observed, accompanied by a nonmonotonic behavior of H_C versus T. More significantly, a phenomenon of decrease (increase) in magnitude of H_E at low (high) T with increasing H_{FC} is first observed in experiment while H_C is always insensitive to H_{FC} below T_B. It is also found that the mechanisms of negative and positive H_E influenced by H_{FC} are quite different. Therefore, the highlight of this paper includes exhibiting the H_{FC} modulation of the T-dependent EB behaviors in SG/FM bilayers experimentally and interpreting these behaviors simultaneously by using a unified vector model.

Methods

Sample fabrication and measurement. The samples were deposited on silicon wafer by DC magnetron sputtering at room temperature with a stacking sequence of Ta(4 nm)/Fe_xAu_{1-x}(50 nm)/FeNi(5 nm)/Ta(2 nm). Here, x denotes the atomic fraction of Iron in FeAu alloy. The FeAu layer was co-sputtered with tilted iron and gold guns and the sample composition was characterized by Energy Dispersive X-Ray Spectroscopy (EDX). By fixing the sputtering power of iron and varying that of Au, x was varied from 4% to 14%. A 4 nm Ta buffer layer was deposited to promote the SG/FM morphology and a 2 nm Ta capping layer was deposited to prevent sample from oxidation. FeNi represents $Fe_{19}Ni_{81}$, which is used as the magnetic pinned layer. The base pressure for sputtering was better than 7.0×10^{-6} Pa and the working Ar pressure was kept at 0.3 Pa during film deposition. Another series of Fe_xAu_{1-x} single layer films with the identical composition and thickness (i.e., 50 nm) were also deposited on Kapton substrates as reference samples for the low-T SG characterization by means of the ZFC and FC M-T measurements.

Magnetic hysteresis loop measurements were performed in a SQUID-VSM (Quantum Design) with the applied magnetic field (in the range from −5 kOe to 5 kOe) parallel to the film plane. Before each M-H hysteresis loop measurement at a specific T, a magnet reset procedure (oscillatory demagnetization between ±1 Tesla) was performed in order to train the sample to an approximately equilibrium state to eliminate the EB training effect and reducing the residual magnetic field to less than 3 Oe. This will ensure that the obtained H_E and H_C are accurate with an error less than 3 Oe.

Theoretical model and calculation details. On atomic scale, the real coarse-grained SG/FM bilayers are simulated by a finite number of spins placed on the nodes of a simple cubic lattice. By means of effective size scaling, a lateral dimension of 40×40 units in the film plane and a film thickness of 5 monolayers are used with periodic boundary conditions only applying in the plane. Simulations were performed with the Heisenberg model, with the Hamiltonian written as

$$\begin{aligned}\mathcal{H} = & -J_{\mathrm{FM}}^{ij} \sum_{<ij\in \mathrm{FM}>} \boldsymbol{\mu}_i \cdot \boldsymbol{\mu}_j - \left(\sum_{i\in \mathrm{FM}} K_{\mathrm{FM}}^{u} \cos \alpha_i{}^2 + \sum_{i\in \mathrm{FM}} K_{\mathrm{FM}}^{s} \cos \beta_i{}^2 \right) - \mathbf{H} \sum_{i\in \mathrm{FM}} \boldsymbol{\mu}_i \\ & - J_{\mathrm{SG}}^{ij} \sum_{<ij\in \mathrm{SG}>} \boldsymbol{\mu}_i \cdot \boldsymbol{\mu}_j - \sum_{i\in \mathrm{SG}} K_{\mathrm{SG}}^{u} \cos \gamma_i{}^2 - \mathbf{H} \sum_{i\in \mathrm{SG}} \boldsymbol{\mu}_i - J_{\mathrm{IF}}^{ij} \sum_{<i\in \mathrm{FM}, j\in \mathrm{SG}>} \boldsymbol{\mu}_i \cdot \boldsymbol{\mu}_j, \end{aligned} \tag{3}$$

where $\boldsymbol{\mu}_i$ denotes the magnetic moment of the spin at site i. The first term describes the direct exchange energy in the FM. The next two terms are the magnetocrystalline and shape anisotropy energies of the FM, where α_i (β_i) is the angle between $\boldsymbol{\mu}_i$ in the FM and the x (z) axis. The fourth term is the Zeeman energy of the FM, where $\mathbf{H}$ is applied along the x axis. From the fifth to seventh term represent the direct exchange, magnetocrystalline anisotropy, and Zeeman energies of the SG. Here γ_i is the angle between $\boldsymbol{\mu}_i$ in the SG and the x axis. And the last term is the interfacial direct exchange energy between FM and SG. Detailed scaling and parameterizing processes have been described in the Supplementary Material B.

The simulation protocol mimics the experimental process. Initially, a cooling process under an H_{FC} is performed on the SG/FM bilayers, where the FM spins are all pointing to the H_{FC} direction and the SG spins are randomly oriented, from $T = 300$ K to a target temperature. Then, an isothermal magnetization is recorded by cycling H from 5 kOe to −5 kOe to extract H_{E} and H_{C}. As for the update of spin state, a *path-related* Metropolis algorithm[29] is adopted during the Monte Carlo simulation, which has been also introduced in the Supplementary Material B in details. This calculation is repeated for 10^4 times per spin to find the equilibrium state of the system, and then an additional 10^5 steps are taken to measure the thermodynamic average of the magnetization. Finally, 200 independent realizations of the disorder are averaged to reduce the statistical errors.

References

1. Angelini, M. C. & Biroli, G. Spin Glass in a Field: A New Zero-Temperature Fixed Point in Finite Dimensions. *Phys. Rev. Lett.* **114,** 095701 (2015).
2. Zintchenko, I., Hastings, M. B. & Troyer, M. From local to global ground states in Ising spin glasses. *Phys. Rev. B* **91,** 024201 (2015).
3. Alonso, J. J. Low-temperature spin-glass behavior in a diluted dipolar Ising system. *Phys. Rev. B* **91,** 094406 (2015).
4. Wang, C., Qin, S.-M. & Zhou, H.-J. Topologically invariant tensor renormalization group method for the Edwards-Anderson spin glasses model. *Phys. Rev. B* **90,** 174201 (2014).
5. Perez, F. A. *et al.* Phase Diagram of a Three-Dimensional Antiferromagnet with Random Magnetic Anisotropy. *Phys. Rev. Lett.* **114,** 097201 (2015).
6. Takahashi, T. & Hukushima, K. Evidence of a one-step replica symmetry breaking in a three-dimensional Potts glass model. *Phys. Rev. E* **91,** 020102 (2015).
7. Wittmann, M., Yucesoy, B., Katzgraber, H. G., Machta, J. & Young, A. P. Low-temperature behavior of the statistics of the overlap distribution in Ising spin-glass models. *Phys. Rev. B* **90,** 134419 (2014).
8. Leuzzi, L., Parisi, G., Ricci-Tersenghi, F. & Ruiz-Lorenzo, J. J. Infinite volume extrapolation in the one-dimensional bond diluted Levy spin-glass model near its lower critical dimension. *Phys. Rev. B* **91,** 064202 (2015).
9. Skumryev, V. *et al.* Beating the superparamagnetic limit with exchange bias. *Nature* **423,** 850–853 (2003).
10. Nogués, J. & Schuller, I. K. Exchange bias. *J. Magn. Magn. Mater.* **192,** 203–232 (1999).
11. Berkowitz, A. E. & Takano, K. Exchange anisotropy—a review. *J. Magn. Magn. Mater.* **200,** 552–570 (1999).
12. Guhr, I. L., Hellwig, O., Brombacher, C. & Albrecht, M. Observation of perpendicular exchange bias in [Pd/Co]-CoO nanostructures: Dependence on size, cooling field, and training. *Phys. Rev. B* **76,** 064434 (2007).

13. Keller, J. *et al.* Domain state model for exchange bias. II. Experiments. *Phys. Rev. B* **66,** 014431 (2002).
14. Nogués, J., Lederman, D., Moran, T. J. & Schuller, I. K. Positive Exchange Bias in FeF_2-Fe Bilayers. *Phys. Rev. Lett.* **76,** 4624–4627 (1996).
15. Hu, Y. & Du, A. The effect of field-cooling strength and interfacial coupling on exchange bias in a granular system of ferromagnetic nanoparticles embedded in an antiferromagnetic matrix. *J. Appl. Phys.* **102,** 113911 (2007).
16. Leighton, C., Nogués, J., Jönsson-Åkerman, B. J. & Schuller, I. K. Coercivity Enhancement in Exchange Biased Systems Driven by Interfacial Magnetic Frustration. *Phys. Rev. Lett.* **84,** 3466–3469 (2000).
17. Gredig, T., Krivorotov, I. N., Eames, P. & Dahlberg, E. D. Unidirectional coercivity enhancement in exchange-biased Co/CoO. *Appl. Phys. Lett.* **81,** 1270–1272 (2002).
18. Kohlhepp, J. T., Wieldraaijer, H. & de Jonge, W. J. M. Onset of magnetic interface exchange interactions in epitaxially grown Mn/Co(001). *J. Mater. Res.* **22,** 569–572 (2007).
19. Nayak, A. K. *et al.* Large Zero-Field Cooled Exchange-Bias in Bulk Mn_2PtGa. *Phys. Rev. Lett.* **110,** 127204 (2013).
20. Sabyasachi, S. *et al.* Glassy magnetic phase driven by short-range charge and magnetic ordering in nanocrystalline $La_{1/3}Sr_{2/3}FeO_{3-\delta}$: Magnetization, M össbauer, and polarized neutron studies. *Phys. Rev. B* **86,** 104416 (2012).
21. Ali, M. *et al.* Exchange bias using a spin glass. *Nat. Mater.* **6,** 70–75 (2007).
22. Yuan, F.-T., Lin, J.-K., Yao, Y. D. & Lee, S.-F. Exchange bias in spin glass (FeAu)/NiFe thin films. *Appl. Phys. Lett.* **96,** 162502 (2010).
23. Ali, S. R. *et al.* Role of interface alloying in the exchange bias of Fe/Cr bilayers. *Phys. Rev. B* **82,** 020402 (2010).
24. Usadel, K. D. & Nowak, U. Exchange bias for a ferromagnetic film coupled to a spin glass. *Phys. Rev. B* **80,** 014418 (2009).
25. Du, J., Zhang, B., Zheng, R. K. & Zhang, X. X. Memory effect and spin-glass-like behavior in Co-Ag granular films. *Phys. Rev. B* **75,** 014415 (2007).
26. Schulthess, T. C. & Butler, W. H. Consequences of Spin-Flop Coupling in Exchange Biased Films. *Phys. Rev. Lett.* **81,** 4516–4519 (1998).
27. Schulthess, T. C. & Butler, W. H. Coupling mechanisms in exchange biased films (invited). *J. Appl. Phys.* **85,** 5510–5515 (1999).
28. Manna, P. K. & Yusuf, S. M. Two interface effects: Exchange bias and magnetic proximity. *Phys. Rep.* **535,** 61–99 (2014).
29. Du, H. F. & Du, A. The hysteresis curves of nanoparticles obtained by Monte Carlo method based on the Stoner-Wohlfarth model. *J. Appl. Phys.* **99,** 104306 (2006).

Acknowledgements

This work was supported by National Basic Research Program of China (Nos. 2014CB921101 and 2010CB923401), National Natural Science Foundations of China (Nos. 51471085, 51331004, 11174131, 11074112, and 11204026), Foundational Research Funds for the Central Universities (No. N130405010), and Informalization Construction Project of Chinese Academy of Sciences during the 11th Five-Year Plan Period (Nos. INFO-115-B01, ZDY2008-2-A12).

Author Contributions

J.D. and Y.H. initiated the study. W.R. prepared the samples by magnetron sputtering. W.R., B.Y. and W.Z. performed the magnetic measurements by SQUID-VSM. Y.H., A.D., M.X. and J.D. analyzed the magnetic results. Y.H. and A.D. developed the theoretical model and did the simulation calculations. Y.H., S.Z. and J.D. prepared the manuscript. All the authors contributed to discussions of the project.

Additional Information

Supplementary information accompanies this paper at http://www.nature.com/srep

Competing financial interests: The authors declare no competing financial interests.

How to cite this article: Rui, W. B. *et al.* Cooling field and temperature dependent exchange bias in spin glass/ferromagnet bilayers. *Sci. Rep.* **5**, 13640; doi: 10.1038/srep13640 (2015).